Trace Elements, Maturation Processes and Diagenesis in Human Deciduous Incisors

Ani Martirosyan * (1), Xavier Jordana (1,2), Judith Juanhuix (3), Marine Cotte (4,5), Nuria Molist (6), Javier Irurita (7), Cristina Santos (1), Assumpció Malgosa (1), Patrick Mahoney (8,9), Judit Molera * (10)

(1) Biological Anthropology Unit, Department of Animal Biology, Plant Biology and Ecology, Faculty of Biosciences, Universitat Autònoma de Barcelona, Cerdanyola del Vallès, 08193 Barcelona, Spain

(2) Tissue Repair and Regeneration Laboratory (TR2Lab), Institut de Recerca i Innovació en Ciències de la Vida i de la Salut a la Catalunya Central (IrisCC), Ctra. de Roda, 08500 Vic, Barcelona, Spain

(3) ALBA Synchrotron Light Facility, Cerdanyola del Vallès, 08290 Barcelona, Spain

(4) European Synchrotron Radiation Facility (ESRF), Grenoble, France

(5) Sorbonne Université, CNRS, Laboratoire d'archeologie moleculaire et structurale, LAMS, F-75005 Paris, France

(6) Museu d'Arqueologia de Catalunya (MAC), 080038 Barcelona, Spain

(7) Department of Legal Medicine, Toxicology and Physical Anthropology, Universidad de Granada, 18071 Granada, Spain

(8) Skeletal Biology Research Centre, School of Anthropology and Conservation, University of

Kent, Canterbury, UK

(9) School of Chemistry and Forensic Science, University of Kent, Canterbury, UK

(10) MECAMAT, Facultat de Ciències, Tecnologia i Enginyeries, Universitat de Vic-Universitat Central de Catalunya, Campus Torre dels Frares, 08500 Vic, Spain

*** Corresponding author**

Ani Martirosyan

Ani.Martirosyan@uab.cat

Judit Molera

judit.molera@uvic.cat

Abstract

Post-mortem alteration of trace elements can complicate the interpretation of original biogenic signals related to diet, environment and enamel maturation processes. This study describes gradients in element concentrations for modern and archaeological deciduous incisor teeth to identify diagenetic variations in specific elements.

Fifteen human deciduous incisors (six modern and nine archaeological) were prepared for synchrotron radiation micro X-ray fluorescence (SR µ-XRF) analysis targeting the minerals Ca, P, and selected trace elements Zn, Fe, Mn, Cu, and Ba. Standard histological methods were employed to produce thin sections. Element concentrations, expressed in parts per million (ppm) and as a ratio of calcium (Ca), were measured from the outer enamel surface (OES), into the enamel, across the Neonatal Line (NNL) and enamel-dentin junction (EDJ), and into the dentin.

Diagenesis was most pronounced on the external surfaces of enamel and dentin, with notable variability in Fe, Mn, Cu, and Ba. In contrast, Ca, P, and Zn levels remained stable across samples, with a slight increase in Zn at the NNL. There was no enrichment of Zn at the OES in enamel not yet matured (less than 33-37 postnatal days), suggesting that initial zinc incorporation is overshadowed by further deposition during maturation.

Diagenetic alteration of the Fe, Mn, Cu, and Ba elements in deciduous incisor enamel appears to affect their concentration in regions of the archaeological teeth. The observed Ca and Zn distribution pattern reflects distinct enamel maturation stages, highlighting the need to consider both diagenetic influences and developmental processes in trace element analyses of ancient dental samples.

1. Introduction

The inorganic fraction of tooth enamel consists mainly of apatite crystals of Ca and P with small amounts of trace elements. Histologically controlled trace element analysis is increasingly utilized to obtain information about the diet and environment of ancient humans and fossil hominins (Humphrey, 2014; Humphrey et al., 2008; Kubat et al., 2023; Lugli et al., 2019). Enamel is often utilized for this purpose as it is less susceptible to diagenetic change compared to bone (Hinz & Kohn, 2010; Hoppe et al., 2003). Yet, post-mortem addition of elements from the burial environment, as well as the maturation stage of enamel, can still alter trace element compositions and affect interpretations of the original biogenic signal (e.g., Kamenov et al., 2018; Müller et al., 2019). Previous studies have employed whole crown elemental mapping techniques to analyze the distribution patterns of biogenic elements related to retrospective evidence of the forming enamel front indicated by successive incremental and accentuated growth lines (Austin et al., 2013; Smith et al., 2022). These developmentally informed approaches using laser ablation inductively coupled plasma mass spectrometry (LA-ICP-MS) offer valuable insight into the spatial and temporal variation of chemical elements. Here, we utilize synchrotron radiation micro X-ray fluorescence (SR µ-XRF) (e.g., Dean et al., 2019, 2023). We selected SR µ-XRF as this can provide a finer scale and better detection capabilities of trace elements in teeth compared to LA-ICP-MS (Specht et al., 2025).

This study focuses on human deciduous teeth, which start to form before birth, making them crucial for understanding the pre- and postnatal distribution of elements (Arora et al., 2011, 2012; Dean et al., 2019; Jensen et al., 2023), and for reconstructing diet just after birth (Nava et al., 2020). We map the concentration and distribution of Ca, P, and selected trace elements (Mn, Zn, Fe, Cu, Ba) in samples of human deciduous incisors that date to the 20th century AD and two archaeological periods (Medieval 5th-8th centuries AD; Iberian Iron Age 4th-3rd centuries BC). The aim was to identify variation in elements through time, and to determine whether temporal variation is consistent across all elements. Element concentrations were measured in the dentin, across the enamel dentin junction (EDJ), into prenatal enamel, across the birth neonatal line (NNL) and into the postnatal enamel. Using SR µ-XRF at the ID21 beamline of the European Synchrotron Radiation Facility (ESRF), we achieve ppm-level elemental analysis with a spatial resolution of 1 µm. Element concentrations were expressed as ppm, and as a ratio of Ca.

1.1 Enamel formation

Enamel formation commences in human central deciduous incisors in the second trimester of pregnancy and continues in deciduous second molars until early in the second year after birth (Mahoney, 2015). Formation is conducted in two stages by enamel forming cells, named ameloblasts (Boyde, 1997). In the first secretory stage, ameloblasts secrete a protein-rich matrix primarily composed of amelogenin, along with smaller quantities of other proteins. Within this matrix, inorganic hydroxyapatite (HA) crystals, consisting of calcium and phosphate, are deposited (Nanci, 2018). As enamel formation progresses, the crystals are organised into rods by the distal portion of ameloblasts, named Tomes process (Simmer et al., 2011). These rods, about 5 µm in width, extend over hundreds of micrometers, from the EDJ towards the future outer enamel surface (Beniash et al., 2019).

In the second stage of enamel formation, named the maturation stage, about 25% of ameloblasts are lost, and the activity of proteins and enzymes changes (Lacruz et al., 2017; Simmer et al., 2012). Enamel prisms elongate and existing crystals widen as proteins are removed from the matrix (Beniash et al., 2019; Josephsen et al., 2010). Proteases such as KLK-4 play crucial roles in degrading enamel proteins during maturation (Beniash et al., 2019; Lu et al., 2008). Thus, a substantial increase in enamel mineralisation takes place during the maturation stage of enamel growth (Humphrey, 2014).

Enamel formation follows a circadian rhythm, producing daily incremental markings known as enamel cross-striations (Zheng et al., 2013, 2014) that are routinely drawn upon in studies of enamel histology Antoine et al., 2009; Kierdorf et al., 2021; Macchiarelli et al., 2006; McFarlane et al., 2021; Witzel et al., 2008). Systemic disturbances, such as birth, can alter enamel secretion, leading to the formation of Accentuated Lines (ALs). The NNL is a distinctive AL that typically appears in the enamel of human deciduous teeth during birth or shortly afterward (Mahoney, 2011, 2012; Nava et al., 2017).

1.2 Element incorporation into forming enamel

Trace elements can enter the human body through food, water or the environment (Bentley, 2006). The mineral component of enamel and dentin is a type of biological apatite in the form of carbonated hydroxyapatite ($Ca_{10}(PO_4)_6(OH)_{2-x}(CO_3)_x$.). Biological apatite contains trace elements in small quantities that are incorporated during the secretion and maturation stages of mineralization (Pajor et al., 2019; Shaik et al., 2021; Sharma et al., 2020). Different element ions, such as Mg^{2+}, K^+, Na^+, Zn^{2+}, Mn^{2+}, SiO_4^{4-} and Cl^-, can either substitute for Ca, P, or hydroxyl ions in the HA crystal structure, or reside within the hydrated surface layer of the crystals (Hughes and Rakovan, 2015; Pajor et al., 2019; Sarna-Boś et al., 2022). For example, manganese (Mn) replaces Ca in the hydroxyapatite structure, occupying specific sites within the crystal lattice (Liu et al., 2021; Mayer et al., 2010). Similarly, iron (Fe2+) and copper (Cu2+) incorporate into HA by occupying positions within the hexagonal channels of the structure (Saito et al., 2023).

Zinc (Zn^{2+}) can substitute for calcium (Ca^{2+}) in the HA of teeth and bones (Hughes and Rakovan, 2015; Pajor et al., 2019; Sarna-Boś et al., 2022). The substitution influences tooth mineralization and enzyme activity related to tissue maintenance and repair (Müller et al., 2019). Zn distribution in enamel reflects the composition if mineral formed during both early secretory and late maturation phases (Dean et al., 2023; Hubbard, 2000). Fluctuations in Zn concentrations follow the incremental formation pattern of teeth (Dean et al., 2023; Donangelo and King, 2012; Terrin et al., 2015).

1.3 Previous research on the distribution of trace elements in human teeth

The study of Zn in relation to the NNL has offered insights into developmental processes associated with birth. Dean et al. (2019) utilized SXRF to analyzed Zn and Ca in erupted deciduous canines and molars, identifying a distinct peak in Zn at the NNL. This peak was related to high Zn concentrations during early lactation, independent of maternal diet, and a reduced and disordered crystallinity. Their subsequent work in primates, including Neandertal specimens, revealed consistent peaks in Zn at the NNL, that was linked to a high Zn content in colostrum and release of this element at birth (Dean et al., 2023). Additionally, they observed a significant Zn enrichment at the outer enamel surface (Dean et al., 2023). This supports earlier findings that KLK-4, a key enzyme in enamel maturation with Zn binding motifs, accumulates at the enamel

surface during matrix degradation, explaining an increase in Zn towards the OES (Müller et al., 2019). In a previous study, we analyzed Zn, Ca, and Cu distributions to examine the relationships of the NNL to these elements (Martirosyan et al., 2024). Other have using LA-ICP-MS to revealing variations in elements such as Ba and Zn across the NNL, which was used to reconstruct birth and nursing histories in human and non-human primate dental samples (e.g., Austin et al., 2013; Smith et al., 2023).

Using atomic absorption spectrophotometry, Fosse and Justesen (1978) observed that Cu concentrations in deciduous teeth vary significantly between urban and rural environments, underscoring the influence of environmental exposure during early development. Unlike Cu, Zn concentrations in teeth show greater stability across different geographical contexts (Fosse and Justesen, 1978). Research by Derise and Ritchey (1974) reported that while elements like Pb, Mn, Cu, Zn, and Sr concentrate in the enamel, other elements such as Fe and F are more abundant in dentin.

Dantas et al (2020) and Sabel et al. (2008) explored mineral distribution in exfoliated primary deciduous teeth using quantitative birefringence and SEM, respectively. Sabel et al. (2008) found that the highest concentrations of Ca and P occurred at the EDJ, gradually decreasing toward the tooth surface. Dantas et al. (2020), compared prenatal and postnatal enamel, reporting that prenatal enamel was more calcified, less organic, and contained more water than postnatal enamel. Both studies identified hypomineralized NNLs.

1.4 Previous research investigating diagenetic changes in archaeological teeth

Even though teeth are generally more resistant to diagenetic change than bone, certain trace elements that have been incorporated into enamel and dentin are still susceptible to diagenesis after burial (Huang et al., 2023; Kendall et al., 2018; Micó et al., 2024; Rey et al., 2022). Weber et al. (2021) found that dentin is particularly susceptible to changes in Ca, Sr, Zn, and Mn, while enamel generally maintains its original structure. A study of medieval teeth revealed elevated levels of Fe, Ba, Mn, and Pb compared to modern-day samples which was attributed to uptake from the soil during burial (Carvalho et al., 2007). In the same study, Sr and Zn values were generally similar in both the modern and medieval samples suggesting limited diagenetic change in these trace elements (Carvalho et al., 2007). Williams and Siegele (2014) found higher Fe concentrations in medieval enamel, and suggested that the outer enamel layers are more affected by diagenetic change. A similar finding was reported by Kamenov et al (2018) for archaeological samples of teeth, that had increased concentrations of Fe, as well as Mn and rare earth elements. Rey et al. (2022) analysed more ancient fossil enamel, revealing diagenetic alteration involving Sr, Mn, and uranium linked to secondary mineral phases like calcite. Together, these studies demonstrate that burial environments can markedly alter the chemical composition of dental enamel, particularly affecting elements such as Fe and Mn. Understanding these diagenetic processes is crucial for interpreting archaeological data accurately.

2. Materials and Methods

2.1 Samples

Fifteen deciduous incisors (n= 9 central, n= 6 lateral) were selected, representing modern and archaeological samples (Table 1). Six incisors were from the skeletal collection of infants (20th century AD) curated at the Department of Legal Medicine, Toxicology, and Physical Anthropology, of the University of Granada, Spain (Alemán et al., 2012). These individuals were buried in sealed niches, a practice that contributed to the remarkable preservation of their skeletal remains. The age-at-death was known for the six samples (Table 1). The protocol for studying these bone remains was approved by the ethics committee of the University of Granada and complied strictly with national regulations (Law 14/2007, 3rd July) on the protection of personal privacy and confidential treatment of personal data in biomedical research. The remaining incisors were from the recent Early Middle Ages (Sant Pere de Terrassa) and more ancient Iberian Iron Age (Olèrdola). All archaeological samples are unerupted, except for one individual (SPUF68_52) whose age-at-death was estimated to be 1 year after birth (Jordana et al., 2019). All teeth were identified using the FDI World Dental Federation notation (ISO, 2016).

Sant Pere de Terrassa (SP) is a monumental religious complex located in Terrassa, Barcelona (Spain) that includes the Romanesque churches of Santa Maria, Sant Miquel, and Sant Pere. Excavations conducted from 1995 to 2003 revealed that these structures were built over an earlier Visigothic Episcopal cathedral from the fifth to eighth centuries AD (Garcia et al., 2003). The site's necropolis was used continuously from the fourth century to the modern era, providing a well-defined chronology of graves (Jordana et al., 2019). For this study, three incisors from different individuals were analyzed. SPUF396.2 and SPUF582.1 were buried in simple burial pits without a coffin, while SPUF68 was interred in a tegulae coffin made with Roman roof tiles.

Sant Miquel d'Olèrdola (OLE) is an archaeological site in Olèrdola (Alt Penedès, Barcelona, Spain) with evidence of a settlement dating back to the early Iron Age (8th - early 6th centuries BC). Between the 5th and 1st centuries BC, the area was occupied by the Cessetans, an Iberian people of the Catalan coastal region. Excavations revealed intramural inhumations in simple burial pits, containing the remains of at least 11 perinatal individuals, datable to between the mid-fourth century BC and the early second century BC. Six incisors from different individuals in this study originate from this site and were not analyzed by SXRF in our previous publication (Martirosyan et al., 2024).

2.2 Section preparation

Teeth were embedded in ExpoxiCure™ 2 mounting resin (Buehler) and cut along the mid-sagittal plane using a minitom equipped with a diamond cut-off wheel (Struers). One resulting section from each tooth was preserved for synchrotron analysis, while the other was used to obtain thin sections following standard methodologies (Martirosyan et al., 2024). Sections for synchrotron analysis underwent successive polishing steps using diamond suspensions of 6µm, 3µm, 1µm, and 0.25 µm. The histological sections were examined under a transmission petrographic optical microscope equipped with a Leica DM2700 P dual polarisation system at magnifications of 5X, 10X, and 20X, facilitated by Micrometrics SE Premium Software. Photomontages of the images were crafted using MosaicJ (Schindelin et al., 2012).

2.3 Neonatal Line Study and Crown Formation Time

The NNL was identified as the first Accentuated Line (AL) that was visible along a minimum of 75% of its length (FitzGerald & Saunders, 2005). It is typically distinguished from other accentuated lines by its prominence and clear disruption to enamel prisms. The NNL appears as a dark, sharp band against the lighter surrounding enamel when viewed under a light microscope (Hurnanen et al., 2017; Kurek et al., 2016; Zanolli et al., 2011).

To determine the prenatal Crown Formation Time (pCFT) of the incisors, we followed standard methods (e.g., Martirosyan et al., 2024; Nava et al., 2017; Peripoli et al., 2023). A 200 μm line was traced from the EDJ following the pathway of enamel prisms until reaching the NNL (Birch and Dean, 2014; Dean et al., 2020; Mahoney, 2011, 2012). The length of the prisms was divided by mean local daily secretion rates (DSRs), using the 95% confidence interval (CI) for each tooth zone (upper, middle, and lower) to provide maximum and minimum pCFT values. If the NNL is present, chronological age is calculated by measuring the prism length from the EDJ to the enamel surface and dividing by the mean DSR of region at the NNL-EDJ meeting point. If the NNL is absent, tracing continues throughout the entire crown.

2.4 Data acquisition, processing, and analysis of μ-XRF maps

Elemental data were acquired from a path across the thin section that commenced at the OES, traveling across the postnatal enamel, enamel NNL, the prenatal enamel, EDJ, prenatal dentin, dentin NNL (when visible), and postnatal dentin.

μ-XRF maps were acquired at the ID21 beamline of the European Synchrotron Radiation Facility (ESRF) (Cotte et al., 2017). Utilizing an undulator, X-rays were generated, and their energy was precisely calibrated with a Si(311) double-crystal monochromator. To achieve optimal sample analysis, the beam was focused to dimensions of 0.5 μm × 0.9 μm (vertical × horizontal) through the implementation of a Kirkpatrick Baez mirror system. During experimentation, the samples were positioned with an angle of 62° with respect to the incident X-ray beam within a vacuum environment, ensuring controlled conditions for XRF.

To enhance data accuracy, the acquired XRF spectra underwent deadtime correction and correction for beam intensity fluctuations, continuously monitored with a photodiode positioned upstream of the sample. Over the 2D μ-XRF maps, specific points of interest were then identified.

During the initial phase, we generated a preliminary map with a pixel size ranging from 2 to 6 μm. Upon identifying the optimal region where the NNL was distinctly visible, we uniformly adjusted the width of μ-XRF maps to 50 μm and the height such to cover from outside the enamel surface down to beyond the dentin surface (Fig.2). XRF quantification was performed using PyMCA (Solé et al., 2007).

From the mapping obtained by μ-XRF at ID21-ESRF, we generated chemical profiles of P, Ca, Ba, Mn, Fe, Cu, and Zn from the enamel to dentin, perpendicular to the tooth surface. To enhance the interpretability of the graphs and ensure data comparability, the distances of the 1D line scans were normalized (Supplementary Material). In all the samples, position 0 corresponds to EDJ. The NNL of the enamel and dentin was standardized to -50 and 50 (arbitrary unit), respectively, with the OES set at -100. Not all samples included data extending to the outer dentin surface (ODS). Thus, this postnatal dentin region was

not normalized. For archaeological samples, the enamel NNL was positioned at -50. When a visible NNL in the dentin was absent, normalization was not applied at this point. In these cases, data were available up to the OES (-100) and the ODS (100).

Although Ca and P are not trace elements. They were included in the analysis as reference components of the hydroxyapatite matrix. Their inclusion helps contextualize the relative distribution and signal intensity of elements with lower concentrations such as Zn or Ba. To facilitate comparison across sample types, average concentrations of each element were calculated for modern (n=5), Sant Pere de Terrassa (n=2), and Olèrdola samples with (n=2) and without (n=5) NNL. Due to the high variability in iron concentration in the archaeological samples, individual values were used for this element to ensure a more accurate representation in the graphs. Enamel thickness was thinner in Olèrdola samples compared to those from Sant Pere de Terrassa, as they are at an earlier stage of enamel formation. Therefore, the data were analyzed separately for each site.

Graphs were created in Excel, and all statistical analyses to investigate correlations were performed using R (R Core Team, 2022).

3. Results

3.1 Histological and Elemental Analysis

A neonatal line was present in the enamel of n=6/6 modern incisors, n=2/3 of the Sant Pere de Terrassa incisors, and n=2/6 of the Olèrdola incisors. Five archaeological samples did not have NNLs, and two were likely preterm births (OLE03 and OLE07). This assumption is based upon the absence of root growth in these five samples, and relatively short crown formation times (Table 1). Table 2 provides the mean values and standard deviations for the concentrations of P, Ca, Mn, Zn, Fe, Cu, and Ba in the modern and archaeological samples.

Table 1: Samples. Provenance, chronology, ID_Tooth (sample identification), and tooth used in this study (FDI nomenclature), minimum and maximum confidence intervals (CI) for prenatal crown formation time (pCFT) in days, minimum and maximum confidence intervals (CI) for histological age in days*, presence of Neonatal Line (NNL), and known age at death for modern samples.

Provenance	Chronology	ID_Tooth	Tooth	pCFT in days (CI min - CI max)	NNL presence	Histological postnatal days (CI min - CI max)	Known Age at Death (days)
Olèrdola Site[1]	350 to 200 BC	OLE01_62	62	164-190	Yes	20-24	-
		OLE03_81	81	106-115	No	0	-
		OLE04_61	61	163-186	Yes	9-10	-
		OLE06_81	81	117-134	No	0	-
		OLE07_61	61	93-101	No	0	-
		OLE08_71	71	145-159	No	0	-
Sant Pere de Terrassa Site[2]	5th - 10th centuries AD	SPUF396.2_71	71	156-182	No	0	-
		SPUF582.1_61	61	168-183	Yes	33-37	-
		SPUF68_52	52	161-177	Yes	67-74*	-
University of Granada[3]	20th century AD	G190_72	72	158-186	Yes	62-74*	263
		G200_72	72	154-175	Yes	44-48*	579
		G308_81	81	198-227	Yes	59-65*	164
		G380_61	61	156-179	Yes	77-90*	116
		G393_52	52	135-147	Yes	78-89*	91
		G414_61	61	158-174	Yes	45-53*	78

1= Subirà and Molist (2007). 2= Jordana et al. (2019). 3= Alemán et al. (2012)

* The known age-at-death is later than the histological age. Histological postnatal days shows the crown formation time, not the age-at-death.

3.2 Calcium, phosphorus and zinc

The mean concentration of calcium and phosphorus in the modern samples is greater in enamel than in dentin, with the greatest enrichment of both Ca and P occurring at the EDJ (Fig. 1; see Supplementary Material for individual profiles from XRF maps for each of the n=5 incisors). Both elements exhibit a generally consistent concentration from the OES to the prenatal enamel, increasing towards the EDJ. There is a decrease in calcium across the enamel NNL by a mean of 16165 ppm, compared with prenatal enamel, followed by a slight increase of 3413 ppm in postnatal enamel. The mean concentration of Ca and P is slightly higher in prenatal compared to postnatal dentin (Table 2).

The outermost enamel is zinc-rich, with a substantial decrease in the concentration of Zn in enamel towards the NNL (Fig. 1, blue line). However, a slight enrichment of Zn is observed at the enamel NNL. The mean concentration of Zn in prenatal enamel remains stable and is lower than in dentin. Zinc enrichment rises steeply towards the EDJ and rises again in prenatal dentin before declining into postnatal dentin. A slightly greater enrichment (relative to enamel) occurs across the dentin NNL, with an increase of 20 ppm and 41 ppm compared to the prenatal and postnatal dentin, respectively. These Zn distribution patterns in modern samples are illustrated in Figure 2, which shows Zn XRF maps of both modern and archaeological teeth.

The distribution of calcium and phosphorus in the postnatal enamel of the Sant Pere samples is similar to the modern samples (Fig. 1b). The EDJ is enriched in both elements relative to the enamel, though the increase in concentration is not as great as that observed in the modern samples. On average, dentin shows a lower concentration of both elements compared to enamel, which is similar to the modern samples.

However, unlike the modern samples, there are regions of dentin that display steep increases and decreases in concentration that might be due to an edge effect, coinciding with fracture zones of the sample.

Table 2: Mean values and standard deviations (shown in brackets) are presented in parts per million (ppm) for Ca, P, Zn, Fe, Mn, Cu, and Ba. Data correspond to modern samples from the University of Granada (modern samples with NNL), Sant Pere de Terrassa with NNL (SP), Olèrdola with NNL (OLE), and combined archaeological samples without NNL (SP+OLE without NNL). The calcium-to-element ratios for each of these elements are provided in Supplementary Material.

Element	Sample type	Enamel			EDJ	Dentin		
		Postnatal Enamel	Enamel NNL	Prenatal Enamel		Prenatal Dentin	Dentin NNL	Postnatal Dentin
Ca	Modern	354443 [5045]	351030 [6479]	367195 [17944]	425500 [29173]	337989 [7598]	332359 [2664]	330677 [1992]
	SP with NNL	363557 [8333]	348916 [4446]	357931 [6284]	344149 [35182]		337893 [21127]*	
	OLE with NNL	441575 [21090]	453669 [4157]	422272 [11634]	394149 [33354]		359050 [7749]*	
	SP+OLE without NNL			359873 [19667]	382232 [2723]	363141 [10937]		
P	Modern	258611 [3677]	259359 [5333]	264459 [6916]	294447 [14573]	231796 [6143]	227260 [4757]	228069 [4306]
	SP with NNL	217768 [5344]	218502 [5502]	232258 [11000]	216048 [33062]		203309 [18413]*	
	OLE with NNL	186582 [10189]	213465 [6978]	241759 [23135]	234277 [26810]		206084 [6620]*	
	SP+OLE without NNL			214727 [25179]	243413 [6079]	207357 [12815]		
Zn	Modern	311 [198]	140 [4]	130 [5]	236 [77]	284 [26]	248 [6]	231 [6]
	SP with NNL	315 [78]	243 [18]	195 [10]	213 [38]		259 [24]*	
	OLE with NNL	746 [97]	902 [20]	702 [108]	526 [9]		562 [30]*	
	SP+OLE without NNL			466 [45]	461 [10]	499 [46]		
Fe	Modern	521 [128]	359 [8]	302 [36]	158 [12]	118 [15]	112 [2]	112 [4]
	SP with NNL	1179 [613]	2834 [1766]	1016 [585]	519 [158]		345 [177]*	
	OLE with NNL	5869 [1148]	2853 [530]	1271 [449]	439 [37]		380 [130]*	
	SP+OLE without NNL			1343 [800]	469 [95]	816 [928]		
Mn	Modern	43 [4]	51 [4]	51 [6]	71 [9]	52 [4]	50 [2]	48 [4]
	SP with NNL	159 [146]	110 [61]	92 [38]	121 [64]		89 [22]*	
	OLE with NNL	259 [36]	247 [20]	157 [50]	66 [15]		50 [10]*	
	SP+OLE without NNL			113 [35]	83 [4]	75 [11]		
Cu	Modern	53 [2]	52 [3]	51 [3]	45 [2]	51 [2]	53 [1]	53 [3]
	SP with NNL	64 [5]	68 [5]	69 [7]	75 [8]		94 [5]*	
	OLE with NNL	101 [9]	101 [10]	76 [12]	60 [5]		68 [5]*	
	SP+OLE without NNL			80 [6]	67 [5]	78 [8]		
Ba	Modern	1216 [79]	1038 [57]	1277 [168]	1555 [215]	1066 [92]	1142 [56]	1115 [83]
	SP with NNL	1509 [130]	1578 [111]	1411 [126]	1298 [160]		1327 [154]*	
	OLE with NNL	2922 [148]	2588 [201]	2037 [254]	1672 [127]		1495 [129]*	
	SP+OLE without NNL			1405 [97]	1460 [78]	1424 [100]		

*These samples lacked a visible NNL, preventing prenatal and postnatal dentin differentiation. As a result, the data represents the entire dentin.

There are different levels of calcification in the enamel of the Olèrdola incisors, which were not observed in the modern incisors (Fig.1c). There are generally higher levels of Ca in the postnatal enamel, followed by a steep decrease in concentration after the neonatal line. Both Ca and P show an increased concentration towards the EDJ.

The archaeological samples without the NNL show a gradient of increasing concentration of both Ca and P towards the EDJ (Fig.1d), but there is no discernible peak in these values at the EDJ. The lowest P levels occur at the OES, which was also observed in the Olèrdola incisors.

The Zn distribution pattern in the enamel and dentin of the Sant Pere de Terrassa samples with a NNL closely mirrors that of modern samples, showing a marked decrease in concentration approaching the NNL (Fig. 1b, blue line). In contrast, the Olèrdola samples, which have a lower chronological age, do not follow this trend (Fig. 1c, blue line). Instead, they display a significant increase in Zn concentration towards the NNL, followed by a decline towards the EDJ. Interestingly, the average Zn concentration in the modern and Sant Pere de Terrassa samples is 307 ppm and 256 ppm, respectively, while Olèrdola samples exhibit a much higher average of 746 ppm.

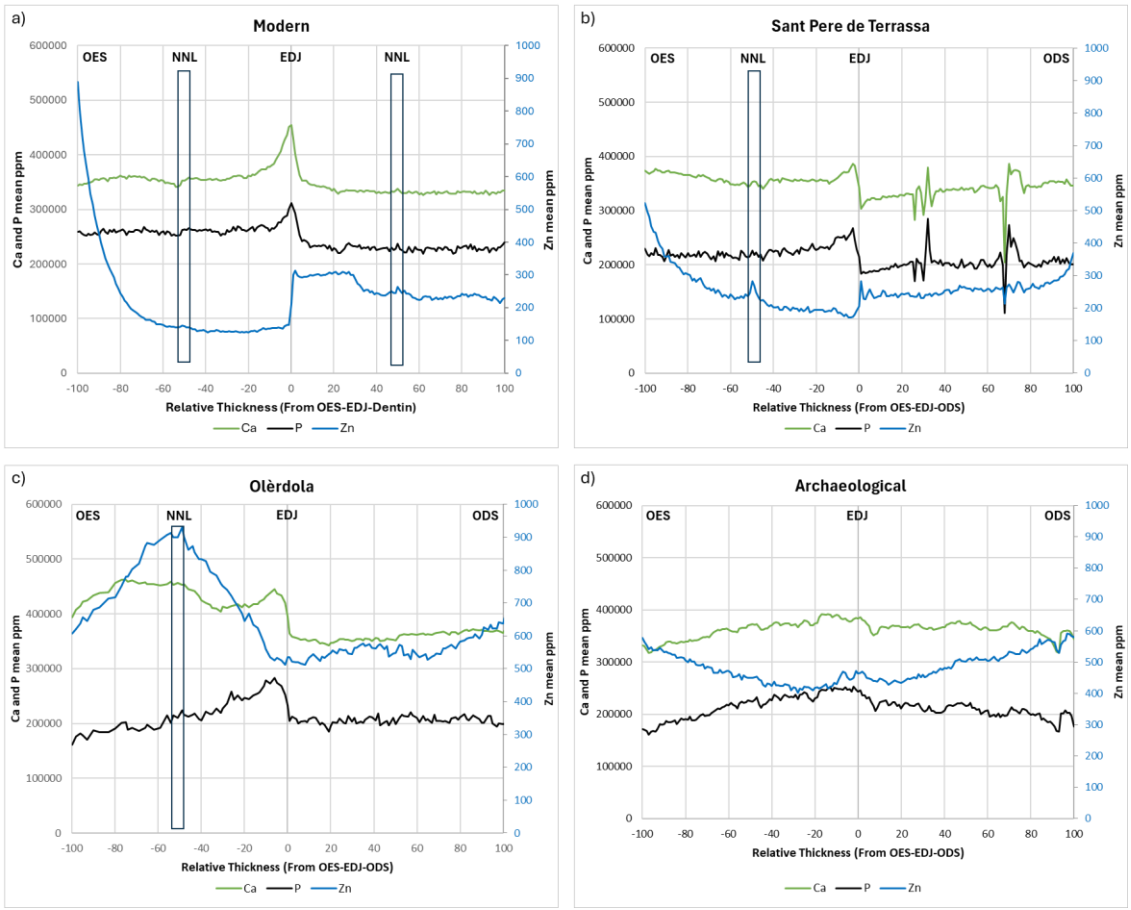

Fig. 1 SXRF 1D line scans of mean calcium, phosphorus and zinc distribution from the outer enamel surface (OES to the left), the EDJ to the dentin or ODS (ODS, near pulp chamber to the right) in a) n=5 modern deciduous incisors, b) n=2 Sant Pere de Terrassa (SP) samples with NNL, c) n=2 Olèrdola (OLE) samples with NNL, d) n= 5 archaeological (SP+OLE) samples without NNL. NNL= neonatal line. The individual profiles from XRF maps for each incisor are in the Supplementary Material.

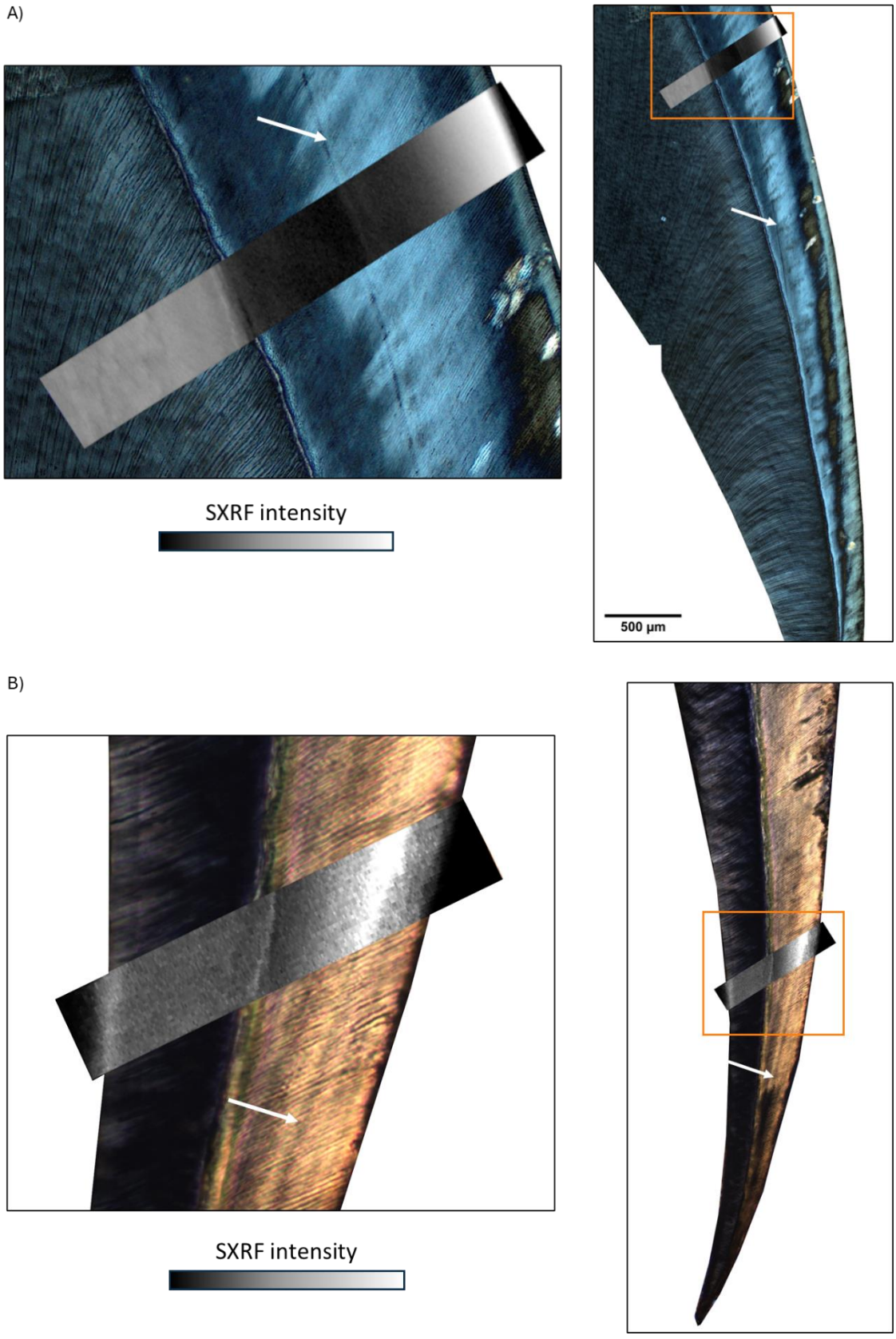

Fig 2. Zinc SXRF maps: A) Modern lower deciduous incisor (sample G-190) and B) Archaeological upper deciduous incisor (sample OLE04), merged with a detailed histological image at 10x magnification. The amplification of the histological image is shown on the left. Enamel neonatal lines (NNL) are indicated by arrows.

Profiles were normalized by relative enamel thickness, meaning that the OES represents the left side of the profile regardless of the final crown thickness or the degree of enamel development. Therefore, the OES of teeth that have not completed enamel secretion does not correspond to the OES of teeth with fully formed crowns. In Figure 3, the distribution of Zn across archeological teeth at various stages of development is depicted, corresponding to survival times of 10, 22, 35 days, during which the crowns are still forming, and more than 1 year, when the crown is fully formed. In the individual that survived 10 days after birth, the Zn profile in the enamel shows a pronounced broad increase around the NNL. In the individual that survived ~22 days, this broad increase is still present but becomes less intense. In the individual that survived ~35 days, the Zn profile becomes relatively flat but retains a sharp peak at the NNL. Finally, in the individual with 1 year of survival, a clear diffusion profile of Zn is observed, extending from the OES towards the EDJ, with a distinct Zn peak at the NNL. The Zn content is higher in the enamel of teeth that have survived fewer days. Regarding the EDJ, there is a marked increase in Zn at 1 year, whereas the increase is less pronounced at 35 and 22 days, and no Zn peak is observed at the EDJ in the 10-day-old tooth. Slightly different patterns are also observed in the distribution of Zn in the dentin. Fig. 3 shows no enrichment of Zn at the OES in enamel that has not reached the maturation process (less than 33-37 days), showing that the initial input of zinc appears to be overprinted by more zinc in the outer enamel during the maturation process for the child who lived till one year.

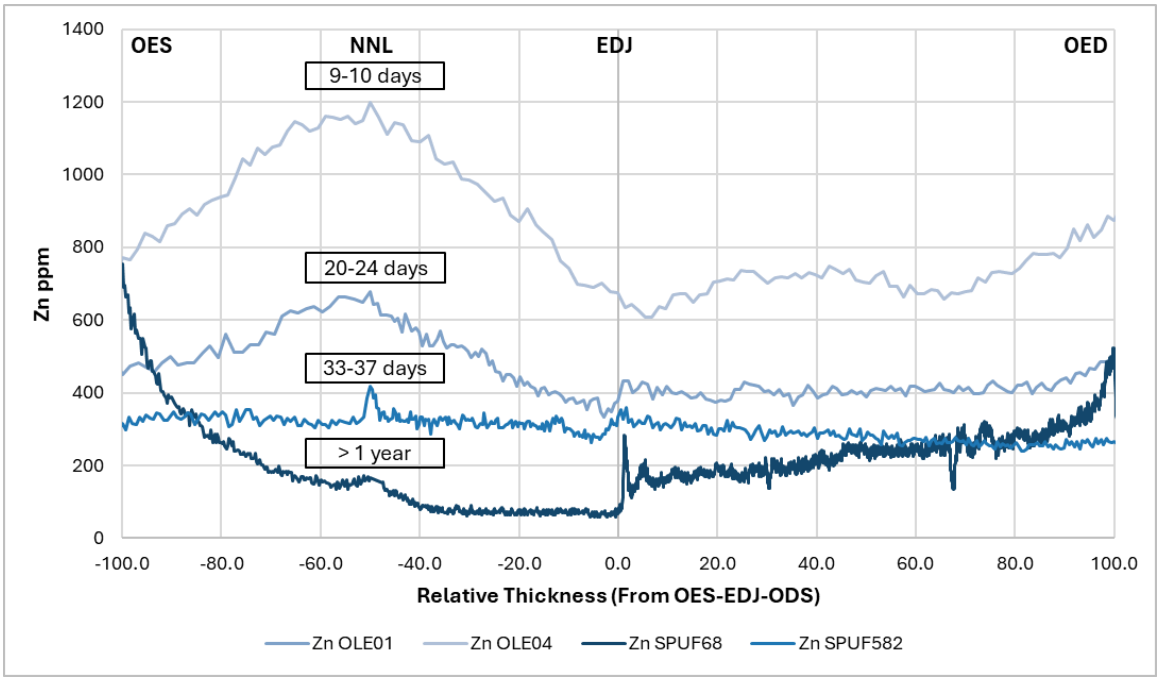

Fig 3. SXRF 1D line scans of zinc distribution from the outer enamel surface (OES to the left), the EDJ to the dentin or ODS (ODS, near pulp chamber to the right) in n=4 archeological deciduous incisors with NNL. Age of each individual is represented in a box, with OLE04 = 9-10 days, OLE01= 20-24 days, SPUF582= 33-37 days, and SPUF68 > 1 year.

3.3 Iron

As with zinc, the highest concentration of iron occurs at the OES followed by a gradual decline in ppm across the NNL and prenatal enamel, with the lowest values occurring in dentin (Fig. 4a). There is a

substantial decrease in Fe from the mean prenatal enamel value of 302ppm to 158ppm at the EDJ (Fig. 5a). The mean NNLs are not enriched or depleted in iron relative to either the enamel or dentin side.

The iron concentration in the enamel of the SPUF68 sample follows the same pattern as the modern samples, with similar Fe content, while OLE04 shows the same trend but at higher concentrations (Fig. 4b and c; refer to the individual profiles in the Supplementary Material for a clearer view of lower values). The other samples have anomalous iron contents with very pronounced peaks that appear to correspond to contamination during burial. In these samples, the concentration is elevated almost ten times higher, with values reaching ~8000 ppm (Fig. 5a). This is further illustrated by the Fe ratios in postnatal enamel (Supplementary material). Iron values close to the enamel NNL of Sant Pere de Terrassa samples show two peaks, one of 3951 ppm and the other of 6725 ppm. In the more ancient Olèrdola samples with NNL, the highest concentration of Fe occurs in the postnatal enamel, closer to the OES, with a mean value of 7970 ppm.

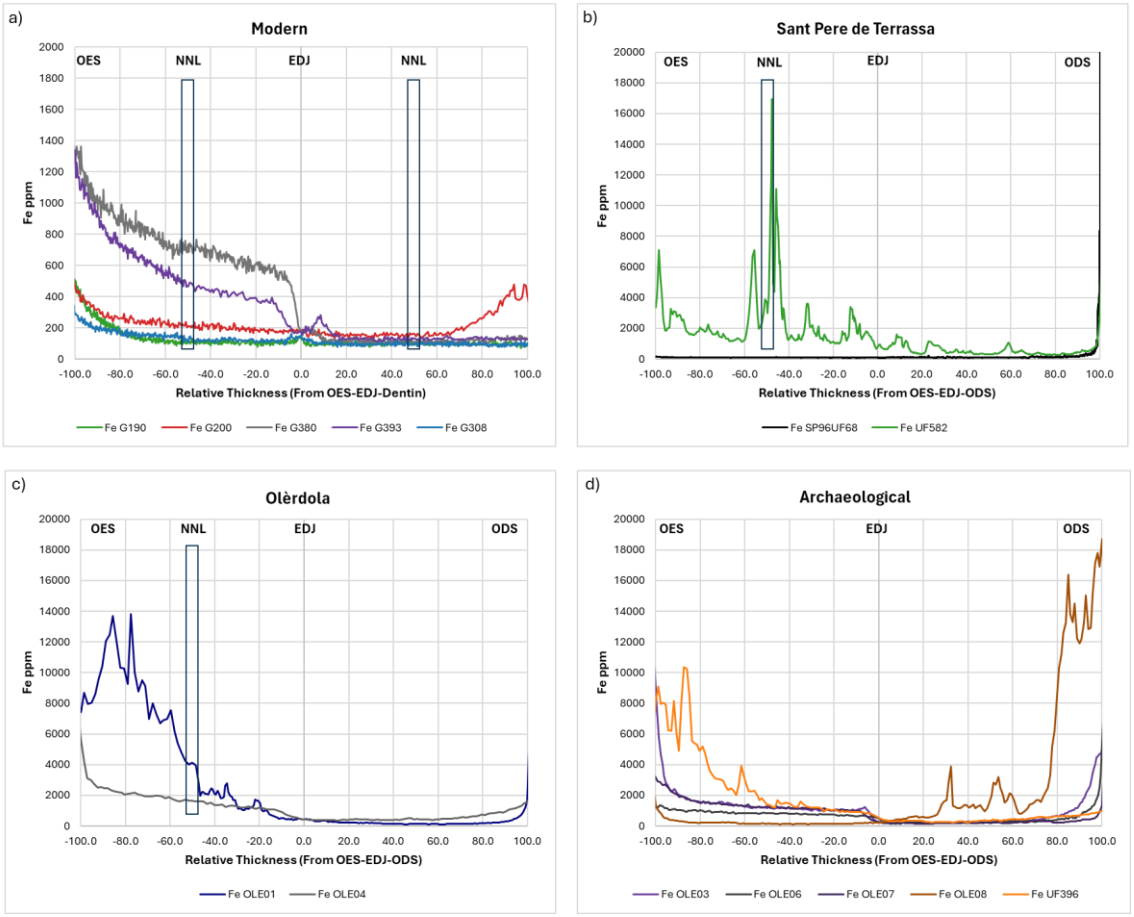

Fig. 4 SXRF 1D line scans of mean iron distribution from the outer enamel surface (OES to the left), the EDJ to the dentin or ODS (ODS, near pulp chamber to the right) in a) n=5 modern deciduous incisors, b) n=2 Sant Pere de Terrassa (SP) samples with NNL, c) n=2 Olèrdola (OLE) samples with NNL, d) n= 5 archaeological (SP+OLE) samples without NNL. NNL= neonatal line.

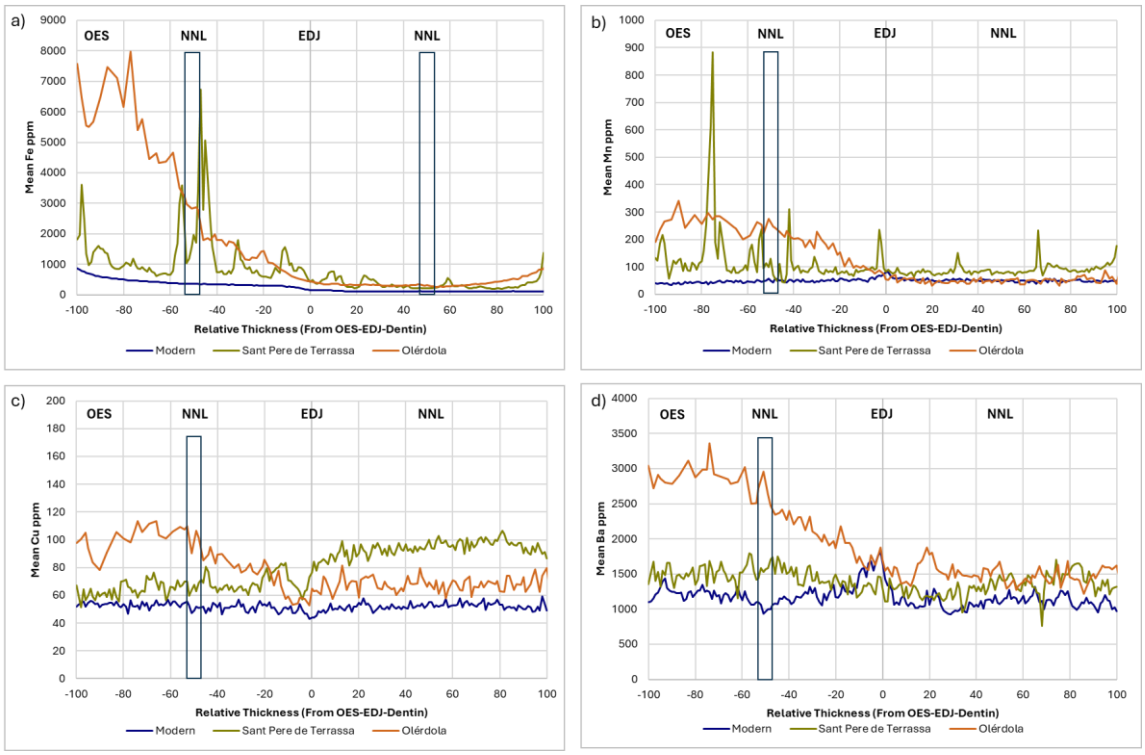

Fig 5. Graphical representation of the mean 1D line scans across modern, medieval (Sant Pere de Terrasa) and Iberian (Olèrdola) deciduous incisors, illustrating the enamel (left in the respective graphs) and dentin (right in the respective graphs) as well as the NNL in the enamel for a) Fe, b) Mn, c) Cu and d) Ba.

3.4 Manganese and Copper

The concentration gradient in enamel for Mn contrasts with the gradient observed for Cu. The graph indicates that Mn concentration decreases postnatally, while Cu concentration increases, suggesting distinct changes in elemental incorporation after birth (Fig. 6a).

Postnatal enamel and dentin exhibit lower Mn values compared to prenatal levels, with a slight enrichment observed at both NNLs and the highest concentrations at the EDJ (Fig. 6, orange line). Cu postnatal enamel values surpass prenatal enamel levels, with a decline at the EDJ, and remaining stable in dentin (Fig. 6, purple line).

Mn and Cu concentration values in archaeological samples follow a different pattern compared to the modern samples, with the archaeological samples showing generally higher values (Fig. 6b, c, and d). Mn in enamel is characterized by a decrease towards the EDJ and numerous concentration peaks. An increase in Cu is observed in the postnatal enamel compared to prenatal enamel in Olèrdola samples with NNL (Fig. 6c, blue line), but this pattern is not seen in Sant Pere de Terrassa samples (Fig. 6 b, purple line).

The concentration of both Mn and Cu are higher in the archaeological samples, with values reaching ~900 ppm and ~110 ppm, respectively (Fig. 5c and d). This trend is reflected in the elemental ratios in postnatal enamel, which increase from 0.00012 for Mn and 0.000152 for Cu in modern incisors to 0.0006 and 0.0002, respectively, in the medieval Sant Pere de Terrassa samples, and further to 0.0007 and 0.0003 in the older Iberian incisors (see Supplementary Material).

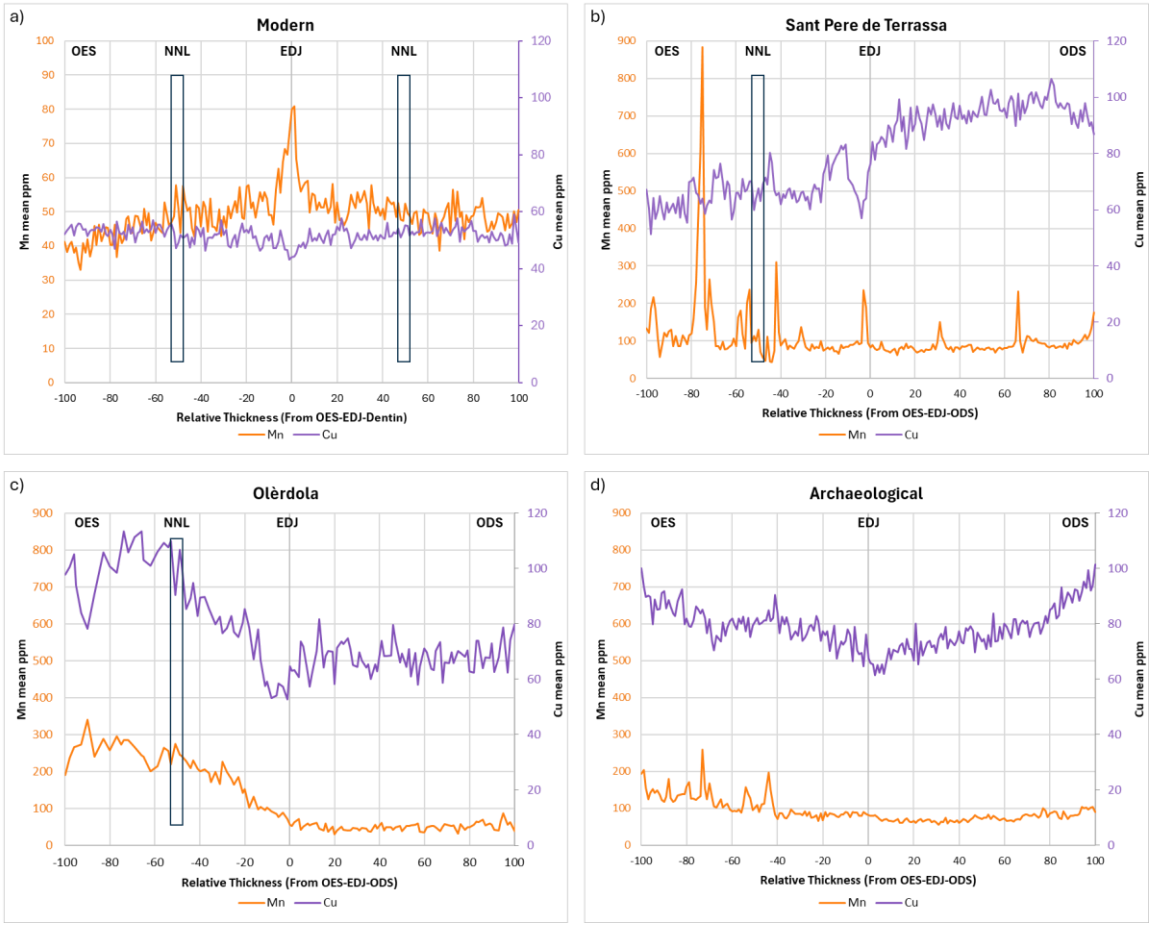

Fig. 6 SXRF 1D line scans of mean manganese and copper distribution from the outer enamel surface (OES to the left), the EDJ to the dentin or ODS (ODS, near pulp chamber to the right) in a) n=5 modern deciduous incisors, b) n=2 Sant Pere de Terrassa (SP) samples with NNL, c) n=2 Olèrdola (OLE) samples with NNL, d) n= 5 archaeological (SP+OLE) samples without NNL. NNL= neonatal line. The individual profiles from XRF maps for each incisor are in the Supplementary Material.

3.5 Barium

The modern samples exhibit a distinct Ba pattern, characterized by a decrease from the OES towards the enamel NNL, followed by an increase towards the EDJ, and then a decrease in the prenatal dentin, followed by a moderate increase in the postnatal dentin. The highest Ba concentration is observed at the EDJ, with a mean value of 1517 ppm (Fig. 5d). A drop in Ba concentration occurs at the enamel NNL, with higher prenatal values compared to postnatal ones, showing an increment of 177 ppm from the NNL to the postnatal enamel. In the dentin, Ba concentrations display a different pattern, with prenatal values lower than postnatal ones. Additionally, there is a significant increase in Ba from the dentin NNL, with a rise of 55 ppm compared to prenatal dentin.

A notable difference was observed between Sant Pere de Terrassa and Olèrdola samples. The concentration is elevated in the archaeological samples with values reaching ~3300 ppm (Fig. 5d). The Ba/Ca ratios in postnatal enamel increase from 0.0035 in modern incisors to 0.005 in the medieval Sant Pere de Terrassa samples, and further to 0.007 in the older Iberian incisors (see Supplementary Material).

The Ba concentration in Sant Pere de Terrassa samples shows values similar to modern samples, ranging from approximately 600 ppm to 1800 ppm. However, the distribution of the element differs from the modern samples. There is an increase from the OES to the NNL in the enamel, followed by a subsequent decrease until the EDJ. In the dentin, the pattern is similar, with an increase towards the ODS. In contrast, Olèrdola samples exhibit higher Ba concentrations, with values peaking at 3358 ppm in the postnatal enamel and reaching a lower value of 1219 ppm in the dentin. In these samples, Ba concentration steadily decreases until the EDJ, where it then stabilizes in the dentin with occasional peaks.

3.6 Neonatal Line

There is a decrease in Ca, P, and Ba at the enamel NNL compared to the prenatal enamel, with reductions of ~27,556 ppm, ~16,585 ppm, and ~385 ppm, respectively (Fig. 2 and 5d). Additionally, the Fe/Ca ratios in samples G-308_72 and G-393_52 indicate Fe enrichment (see Supplementary Material).

Both the Sant Pere de Terrassa and Olèrdola samples show a decrease in P and an increase in zinc at the NNL (Fig. 2b and c, and Fig.3b and c). The findings for calcium are mixed in that the Sant Pere de Terrassa samples exhibit no discernible peak in concentration, whereas Olèrdola samples demonstrate an increase (Fig. 2b and c). Those samples with observable NNL samples show higher enrichment of Zn at the enamel NNL compared to modern samples, with increases of 48 ppm and 200 ppm, respectively, whereas no changes in Zn are observed in archaeological samples without NNL (Fig. 3b and c).

4. Discussion

This study investigated the distribution of trace elements in 15 deciduous incisors from modern and archaeological contexts, focusing on the pre- and postnatal regions of enamel and dentin. Trace elements are incorporated into dental tissues by different mechanisms. Essential elements such as Zn are under tight physiological regulation and play active roles in biomineralization, while others, like Ba, may be passively incorporated or reflect external environmental exposure (Müller et al., 2019, 2024). This distinction is important when interpreting enamel signals, particularly in archaeological contexts where postmortem alteration can further affect non-essential elements (Humphrey et al., 2008; Kamenov et al., 2018).

As expected, our results indicate that enamel is relatively hypercalcified compared to dentin, which is reflected by the higher Ca and P concentrations in both modern and archaeological teeth (Table 2). These results align with the findings of Dean et al. (2019) who reported a significant difference in the distribution of calcium with enamel exhibiting higher calcification levels than dentin. Additionally, we observed higher calcification levels at the EDJ which aligns with previous studies on human teeth (Dean et al., 2019; Sabel et al., 2008).

There were differences in elemental concentrations between prenatal and postnatal enamel. In the Sant Pere de Terrassa and Olèrdola archaeological samples, postnatal enamel exhibited higher Ca concentrations than prenatal enamel. This contrasts with our modern data, where prenatal enamel and dentin are consistently hypercalcified (Fig. 2; see Supplementary Material for individual maps, n = 5 incisors). Dean et al. (2019) found no clear demarcation in calcification between prenatal and postnatal enamel or dentin, whereas Dantas et al. (2020) reported higher calcification in the prenatal enamel of modern samples. These

discrepancies between our modern and archaeological samples may relate to differences in their maturation stage (discussed further below).

Previous studies have concluded that most zinc absorption occurs before eruption, indicated by high Zn levels in unerupted teeth (Brudevold et al. 1963). Similar findings were reported by Dean et al. (2023) who observed a consistent pattern in the distribution of Zn in erupted and unerupted teeth, indicating that Zn levels in external enamel are established before oral exposure and remain stable even after post-mortem diagenetic change. In our modern samples, we found the highest Zn levels in both unerupted (sample G-414_51) and erupted teeth (sample G-190_81). Some of the archaeological samples (OLE01, OLE04, SPUF582, and SPUF396), with crowns that had not completed enamel formation, do not exhibit OES enrichment. Instead, these archaeological samples show higher Zn concentrations at the NNL, except for SPUF396, which lacks a NNL and has its highest Zn concentration in the dentin. The Zn concentration at the OES in the archaeological samples ranges from a minimum of 168 ppm to a maximum of 874 ppm (see Supplementary Material for individual sample values). No differences in OES Zn concentration values were observed between the erupted tooth (SPUF68_52) and unerupted teeth (Fig. 3).

In our archaeological samples, the lowest Zn concentration (59 ppm) was found in the prenatal enamel of SPUF68_52, a fully erupted and mineralized tooth (see Supplementary Material). In contrast, other archaeological samples showed a greater-minimum Zn concentrations of 263 ppm in the prenatal enamel of teeth with a NNL, and a concentration of 234 ppm in teeth without a NNL. The higher Zn concentrations and the lack of Zn enrichment at the OES in unerupted and non-mineralized teeth (Fig.3) may indicate that these teeth have not yet reached the maturation stage of amelogenesis. This stage is crucial for enamel maturation, during which Zn enrichment at the OES may result from residual enzymatic degradation processes (Dean et al., 2023). Zinc accumulation at the OES may reflect its role as a binding group of KLK-4, an enzyme concentrated at the enamel surface during enamel matrix degradation in the maturation stage (Müller et al., 2019; Simmer et al., 2011). Consequently, in those samples that have not yet reached the maturation stage, the enamel matrix would not have degraded, retaining breakdown products and water (Müller et al., 2019; Nanci, 2018). Dean et al. (2023) suggested that Zn enrichment at the EDJ might result from metalloprotease activity during enamel maturation. Our results show a notable Zn concentration increase at the EDJ, particularly in teeth that have undergone maturation (Fig. 3a and b, see Supplementary Material). These observations support the idea of differential Zn distribution linked to developmental stages.

High Zn concentrations were observed in prenatal dentin of modern samples, corroborating findings from other studies (Clark et al., 2023; Dean et al., 2023). Maternal-fetal placental transfer of Zn is an active process, maintaining fetal Zn concentrations higher than maternal levels (Dean et al., 2023). This transfer is crucial during periods of high metabolic demand, like pregnancy and early development (Clark et al. 2023; Chan et al. 1993).

We observed Fe levels in the archaeological incisors were up to ten times higher than in modern samples, which indicates the environment likely served as a significant source for the uptake of this mineral after burial (Fig.5a). Modern teeth displayed Fe enrichment at the OES, decreasing toward the EDJ, while archaeological samples showed multiple peaks throughout the enamel and consistently higher overall Fe

concentrations (Fig. 4). For instance, sample SPUF582.1_61 displays significant peaks, one just after the NNL and another at the NNL, with the latter reaching a remarkable concentration of 16,948 ppm (see Supplementary Material). These peaks are accompanied by a decrease in Ca concentration, suggesting that hypocalcified zones within the enamel may retain more iron from the surrounding soil environment.

The Mn concentrations in our modern samples decreased postnatally (Fig. 6a), which is consistent with other studies that reported Mn absorption is upregulated during early pregnancy but decreases dramatically after birth (Friedman et al., 2022; Jensen et al., 2023). This trend was not observed in the archaeological samples which is probably due to diagenesis, resulting in varying peak concentrations and a higher Mn concentration in the postnatal enamel of these samples (Fig. 6b, c, and d).

The Cu in our modern samples showed a slight postnatal increase of 3 ppm in enamel and 2 ppm in dentin (Fig. 6a). Cu concentrations increase in women's blood during labor due to factors beyond dietary intake, such as increased ceruloplasmin synthesis and elevated maternal estrogen levels (Mbofung and Atinmo 1985; Wasowicz et al. 2001). These levels return to normal shortly after childbirth (Wasowicz et al., 2001). Consistent with our findings, Fischer et al. (2008) reported a moderate (r=0.52) interaction between Mn and Cu in incisors. Again, the archaeological samples exhibited significantly higher Cu levels, up to 110 ppm, likely reflecting a diagenetic contribution (Fig. 6b and c).

Previous research into the distribution of barium in enamel proposed the placenta restricts prenatal barium transfer, but marked enrichment occurs immediately after birth from sources such as maternal milk or infant formulas, which contain higher Ba levels than umbilical cord serum (Austin et al., 2013; and also see Smith et al., 2021, 2022). Consequently, Ba/Ca ratios in enamel and dentin should increase at birth, remain elevated during exclusive breastfeeding, and rise further with the introduction of infant formula (Austin et al., 2013). This proposed variation in Ba/Ca has been supported by various studies (Clark et al., 2023; Smith et al., 2022, 2023). Similarly, studies have shown that in exclusively breastfed infants, Sr/Ca and Ba/Ca ratios decrease until formula and/or solid foods are introduced, whereas in formula-fed infants, these ratios increase until solid foods are introduced (Nava, 2024).

Our findings reveal no change in the concentration of Ba in preterm individuals without a NNL (See Supplementary Material), which is consistent with the restricted transfer of barium by the placenta (Austin et al., 2013). However, our results provide partial support for the predicted postnatal increase in Ba. An increase after birth relative to prenatal enamel was observed in the Olèrdola samples (Fig. 5d). The predicted increase is more variable and less marked in the modern samples and the Sant Pere de Terrassa incisors (Fig. 5d). Variation in Ba content across individuals and lactation stages may contribute to differences in enamel Ba concentrations, as previously reported in modern human and primate samples (Krachler et al., 1999; Smith et al., 2022). Thus, although Ba levels can serve as indicators of early dietary transitions, our results suggest that interpretation of this element in human deciduous enamel must be made cautiously (Fig. 5d).

4. 1 Diagenetic changes in elements

Our investigation reveals that Ca, P, and Zn demonstrate relatively greater stability over time in deciduous enamel compared to the distribution of Fe, Mn, Cu, and Ba which show less consistency on the external surface of the enamel and within the dentin. These latter elements tend to show significant alteration probably due to environmental and post-burial processes, which can affect the reliability of elemental analysis in archaeological contexts (Carvalho et al., 2007; Kamenov et al., 2018; Williams & Siegele, 2014). A recent study using advanced analytical techniques has shown that elements such as Mn, Fe, and Ba can undergo postmortem alteration, particularly through interactions with secondary mineral phases like Fe/Mn oxides or detrital inputs from the burial environment (Müller et al., 2024). They provided a detailed overview of Mn as a highly diagenetic tracer, emphasizing its tendency to form secondary mineral phases such as oxides and carbonates, which often accumulate along exposed surfaces rather than following developmental structures. Our observations of elevated Fe, Mn, and Ba in certain archaeological samples align with these broader patterns of diagenetic overprint.

The availability of different elements in the burial environment, influenced by soil composition and burial practices, may play a significant role in the diagenetic alterations observed. In this study, the SPUF68 sample, associated with an individual buried in a tegula coffin, exhibited Fe, Mn, Cu, and Ba concentrations in enamel that were comparable to modern samples. In contrast, other archeological samples from individuals buried in simple burials displayed more pronounced variations in these elements. Our findings underscore the importance of considering burial practices and soil conditions in future studies to better differentiate between diagenetic changes related to burial conditions and those resulting from enamel maturation processes.

4.2 Neonatal Line

The NNL in the modern and Sant Pere de Terrassa samples showed clear hypocalcification and decreased P levels (Fig. 1a and b), which occurred a few days later than the Zn increment. This may be linked neonatal hypocalcemia, which has an effect 2–8 days after birth (Stimmler et al., 1973). Dean et al. (2019) observed minor Ca reduction at the NNL in a lower deciduous canine, nonetheless, they attributed it to the loss of more friable surface tissue due to the polishing process used in their study. Only samples G308_72 and G393_52 showed hypocalcification at the dentin NNL (see Supplementary Material). The reduction in calcification of the NNL relative to prenatal enamel was not present in the more ancient Olèrdola samples, which may be attributed to the maturation stage of these samples.

Zn enrichment at the NNL was observed but was less pronounced than in Dean et al. (2019). This discrepancy may be attributed to interindividual differences or the fact that deciduous incisors, which were used in this study, complete crown formation earlier compared to the molars and canines (6–11 months) studied by Dean et al. (2019). The earlier completion could result in the OES enrichment being closer to the NNL.

The decrease in Mn after birth in the modern samples could relate to the reduced physiological need for Mn after the prenatal period, during which Mn demand is highest due to rapid fetal growth and development (Bauer et al., 2024; Friedman et al., 2022; Jensen et al., 2023). The reduced Mn after birth was not present

in the archaeological samples, which may be attributed to diagenetic effects altering the Mn composition of the enamel, as manganese has been commonly used as a tracer for postmortem alteration (Kubat et al., 2023; Müller et al., 2024).

Our finding that Ba decreases at the enamel NNL (Fig. 5d) is consistent with other studies (Austin et al., 2013, 2023). However, we have also found an increase in Ba concentration at birth in the Olèrdola samples, similar to that reported by other studies (Clark et al., 2023; Nava et al., 2020). Given these differing results, caution is advised when using Ba levels to identify the NNL or confirm birth events in archaeological samples.

Recent archaeological studies have proposed that postnatal increases in elements such as Ba or Zn near the NNL provide reliable indicators of nursing initiation and neonatal survival (e.g., Dean et al., 2019, 2023; Nava et al., 2024; Smith et al., 2022, 2023). However, our samples did not consistently show the expected postnatal increase in Ba, which is commonly used to trace early-life dietary transitions, particularly in individuals from Sant Pere de Terrassa and the modern reference group. In the case of Zn, its detectability appears to depend on the developmental stage of the tooth, with clearer enrichment patterns emerging only in crowns that have completed the maturation phase. These findings suggest that interpretations based solely on these expected elemental trends should be cautiously approached, especially when enamel formation and diagenetic factors are not fully considered. Postmortem alteration can affect a wide range of trace elements, such as Ba, and distinguishing biogenic signals from diagenetic ones requires careful contextualization of biogenic signals (Müller et al., 2024).

Although linear scanning does not capture the full enamel growth geometry, the profiles in this study offer higher resolution, better elemental sensitivity and are still related to the chronological formation of enamel (ie., prenatal vs postnatal; EDJ vs OES). Our data were acquired from corresponding crown regions and normalized to the EDJ and NNL, enabling cross-individual comparison. While this approach cannot resolve all intra-tooth variation, the patterns align with the expected biological behavior in modern teeth. Variability in archaeological samples is interpreted in relation to both enamel maturation and diagenetic overprint. Future research may benefit from integrating linear profiling of archaeological deciduous teeth with whole tooth mapping to refine spatial interpretations.

5. Conclusion

The distribution patterns of Ca, P, and Zn from the outer enamel surface to the EDJ in modern samples closely resemble those in more recent archaeological samples, suggesting stability in these elements over time. Across all samples, a slight increase in Zn and a decrease in P were observed at the NNL. In the archaeological samples, postnatal enamel had higher Ca concentrations than prenatal enamel, unlike modern teeth, where prenatal enamel is more calcified. These differences may be attributed to incomplete enamel maturation in the archaeological samples, rather than postmortem alteration.

Zinc distribution follows a dynamic, temporally distinct pattern, progressively accumulating from the OES toward the EDJ, with a pronounced Zn peak at the NNL forming as early as 10 days after birth and intensifying into the first postnatal year. This maturation process is characterized by a flattening of the Zn profile at early stages (10–37 days) and a marked Zn enrichment at the EDJ and outer enamel by end of the

first year, suggesting a progressive overprinting of Zn as enamel matures. The distribution of Zn in teeth varies significantly depending on the stage of enamel maturation. In teeth that have not yet matured (less than 33-37 days in deciduous incisors), there is no Zn enrichment at the OES. The absence of Zn enrichment at the OES was only observed in crowns that had not yet completed enamel secretion, indicating that Zn incorporation at the OES occurs during maturation stages. As the enamel matures, particularly in children who lived for one year after birth, the Zn distribution changes markedly. At this stage, a clear diffusion profile of Zn is observed in the enamel, extending from the EDJ towards the OES. This profile includes a distinct peak at the NNL, indicating a significant accumulation of Zn during the maturation process.

Our study reveals that trace elements such as Fe, Mn, Cu, and Ba exhibit higher concentrations in archaeological samples compared to modern ones, with diagenetic effects primarily impacting the outer enamel surface and dentin. This highlights the need for careful interpretation of these elements, as diagenetic changes can obscure biogenic signals.

Acknowledgments

This research was supported by: Ministerio de Ciencia e Innovación (Ref. PGC2018-096666-B-100), Fundación Palarq (call for analysis 2022-2023; PALARQ23_55 Roma a l'Ausetània), Generalitat de Catalunya (GREAB research group, Ref. 2021 SGR 00186). Ani Martirosyan with a fellowship for predoctoral research staff in training (PIF) at UAB. Xavier Jordana is a Serra Húnter Fellow of the Catalan university system. The ESRF is thanked for granting beamtime (HG-224 at ID21).

Data Availability Statement

The authors confirm that the data supporting the findings of this study are available within the article and its Supporting Material.

References

Alemán, I., Irurita, J., Valencia, A. R., Martínez, A., Lõpez-Lázaro, S., Viciano, J., & Botella, M. C. (2012). Brief communication: The Granada osteological collection of identified infants and young children. *American Journal of Physical Anthropology*, *149*(4), 606–610. https://doi.org/10.1002/ajpa.22165

Antoine, D., Hillson, S., & Dean, M. C. (2009). The developmental clock of dental enamel: A test for the periodicity of prism cross-striations in modern humans and an evaluation of the most likely sources of error in histological studies of this kind. *Journal of Anatomy*, *214*(1), 45–55. https://doi.org/10.1111/j.1469-7580.2008.01010.x

Arora, M., Bradman, A., Austin, C., Vedar, M., Holland, N., Eskenazi, B., & Smith, D. R. (2012). Determining fetal manganese exposure from mantle dentine of deciduous teeth. *Environmental Science and Technology*, *46*(9), 5118–5125. https://doi.org/10.1021/es203569f

Arora, M., Hare, D., Austin, C., Smith, D. R., & Doble, P. (2011). Spatial distribution of manganese in enamel and coronal dentine of human primary teeth. *Science of the Total Environment*, *409*(7), 1315–1319. https://doi.org/10.1016/j.scitotenv.2010.12.018

Austin, C., Kumar, P., Carter, E. A., Lee, J., Smith, T. M., Hinde, K., Arora, M., & Lay, P. A. (2023). Stress exposure histories revealed by biochemical changes along accentuated lines in teeth. *Chemosphere*, *329*(March), 138673. https://doi.org/10.1016/j.chemosphere.2023.138673

Austin, C., Smith, T. M., Bradman, A., Hinde, K., Joannes-Boyau, R., Bishop, D., Hare, D. J., Doble, P., Eskenazi, B., & Arora, M. (2013). Barium distributions in teeth reveal early-life dietary transitions in primates. *Nature*, *498*(7453), 216–219. https://doi.org/10.1038/nature12169

Bauer, J. A., Punshon, T., Barr, M. N., Jackson, B. P., Weisskopf, M. G., Bidlack, F. B., Coker, M. O., Peacock, J. L., & Karagas, M. R. (2024). Deciduous teeth from the New Hampshire birth cohort study: Early life environmental and dietary predictors of dentin elements. *Environmental Research*, *256*, 119170. https://doi.org/10.1016/j.envres.2024.119170

Beniash, E., Stifler, C. A., Sun, C. Y., Jung, G. S., Qin, Z., Buehler, M. J., & Gilbert, P. U. P. A. (2019). The hidden structure of human enamel. *Nature Communications*, *10*(1), 1–13. https://doi.org/10.1038/s41467-019-12185-7

Bentley, A.R. (2006). Strontium Isotopes from the Earth to the Archaeological Skeleton: A Review. *J Archaeol Method Theory* **13**, 135–187

Birch, W., & Dean, M. C. (2014). A method of calculating human deciduous crown formation times and of estimating the chronological ages of stressful events occurring during deciduous enamel formation. *Journal of Forensic and Legal Medicine*, *22*, 127–144. https://doi.org/10.1016/j.jflm.2013.12.002

Boyde, A. (1997). Microstructure of enamel. *CIBA Foundation Symposia*, *205*, 18–31. https://doi.org/10.1002/9780470515303.ch3

Brudevold, F., Steadman, L. T., Spinelli, M. A., Amdur, B. H., & Grøn, P. (1963). A study of zinc in human teeth. *Archives of Oral Biology*, *8*, 135–144.

Carvalho, M. L., Marques, A. F., Marques, J. P., & Casaca, C. (2007). Evaluation of the diffusion of Mn, Fe, Ba and Pb in Middle Ages human teeth by synchrotron microprobe X-ray fluorescence. *Spectrochimica Acta - Part B Atomic Spectroscopy*, *62*(6-7 SPEC. ISS.), 702–706. https://doi.org/10.1016/j.sab.2007.02.011

Clark, C. T., Yang, P., Halden, N., Ferguson, S. H., & Matthews, C. J. D. (2023). Patterns of trace element deposition in beluga whale teeth reflect early life history. *Chemosphere*, *340*(August), 139938. https://doi.org/10.1016/j.chemosphere.2023.139938

Cotte, M., Pouyet, E., Salomé, M., Rivard, C., De Nolf, W., Castillo-Michel, H., Fabris, T., Monico, L., Janssens, K., Wang, T., Sciau, P., Verger, L., Cormier, L., Dargaud, O., Brun, E., Bugnazet, D., Fayard, B., Hesse, B., Pradas Del Real, A. E., … Susini, J. (2017). The ID21 X-ray and infrared microscopy beamline at the ESRF: Status and recent applications to artistic materials. *Journal of Analytical Atomic Spectrometry*, *32*(3), 477–493. https://doi.org/10.1039/c6ja00356g

Dantas, E. L. D. de A., de Figueiredo, J. T., Macedo-Ribeiro, N., Oliezer, R. S., Gerlach, R. F., & de Sousa,

F. B. (2020). Variation in mineral, organic, and water volumes at the neonatal line and in pre- and postnatal enamel. *Archives of Oral Biology*, *118*(April), 104850. https://doi.org/10.1016/j.archoralbio.2020.104850

Dean, M. C., Garrevoet, J., Van Malderen, S. J. M., Santos, F., Mirazón Lahr, M., Foley, R., & Le Cabec, A. (2023). The Distribution and Biogenic Origins of Zinc in the Mineralised Tooth Tissues of Modern and Fossil Hominoids: Implications for Life History, Diet and Taphonomy. *Biology*, *12*(12), 1455. https://doi.org/10.3390/biology12121455

Dean, M. C., Humphrey, L., Groom, A., & Hassett, B. (2020). Variation in the timing of enamel formation in modern human deciduous canines. *Archives of Oral Biology*, *114*(April), 104719. https://doi.org/10.1016/j.archoralbio.2020.104719

Dean, M. C., Spiers, K. M., Garrevoet, J., & Le Cabec, A. (2019). Synchrotron X-ray fluorescence mapping of Ca, Sr and Zn at the neonatal line in human deciduous teeth reflects changing perinatal physiology. *Archives of Oral Biology*, *104*(May), 90–102. https://doi.org/10.1016/j.archoralbio.2019.05.024

Derise, N. L., & Ritchey, S. J. (1974). Mineral Composition of Normal Human Enamel and Dentin and the Relation of Composition to Dental Caries: II. Microminerals. *Journal of Dental Research*, *53*(4), 853–858. https://doi.org/10.1177/00220345740530041601

Donangelo, C. M., & King, J. C. (2012). Maternal zinc intakes and homeostatic adjustments during pregnancy and lactation. *Nutrients*, *4*(7), 782–798. https://doi.org/10.3390/nu4070782

Fischer, A., Kwapuliński, J., Wiechuła, D., Fischer, T., & Loska, M. (2008). The occurrence of copper in deciduous teeth of girls and boys living in Upper Silesian Industry Region (Southern Poland). *Science of the Total Environment*, *389*(2–3), 315–319. https://doi.org/10.1016/j.scitotenv.2007.08.046

FitzGerald, C. M., & Saunders, S. R. (2005). Test of histological methods of determining chronology of accentuated striae in deciduous teeth. *American Journal of Physical Anthropology*, *127*(3), 277–290. https://doi.org/10.1002/ajpa.10442

Fosse, G., & Berg Justesen, N. P. (1978). Zinc and copper in deciduous teeth of norwegian children. *International Journal of Environmental Studies*, *13*(1), 19–34. https://doi.org/10.1080/00207237808709801

Friedman, A., Bauer, J. A., Austin, C., Downs, T. J., Tripodis, Y., Heiger-Bernays, W., White, R. F., Arora, M., & Claus Henn, B. (2022). Multiple metals in children's deciduous teeth: results from a community-initiated pilot study. *Journal of Exposure Science and Environmental Epidemiology*, *32*(3), 408–417. https://doi.org/10.1038/s41370-021-00400-x

Garcia Llinares, G. M., Moro i García, A., & Tuset i Bertran, F. (2003). De conjunt paleocristià i catedralici a conjunt parroquial. Transformacions i canvis d'ús de les esglésies de Sant Pere de Terrassa. Segles IV al XVIII. *Terme*, *18*, 29–58. http://www.raco.cat/index.php/Terme/article/view/40822

Hinz, E. A., & Kohn, M. J. (2010). The effect of tissue structure and soil chemistry on trace element uptake

in fossils. *Geochimica et Cosmochimica Acta*, *74*(11), 3213–3231. https://doi.org/10.1016/j.gca.2010.03.011

Hoppe, K. A., Koch, P. L., & Furutani, T. T. (2003). Assessing the preservation of biogenic strontium in fossil bones and tooth enamel. *International Journal of Osteoarchaeology*, *13*(1–2), 20–28. https://doi.org/10.1002/oa.663

Huang, F., Fu, Y., Li, D., Peng, J., He, W., Li, S., Sun, X., & He, G. (2023). Early diagenetic REE migration from Fe-Mn nodules to fish teeth in deep sea sediments. *Ore Geology Reviews*, *160*(July). https://doi.org/10.1016/j.oregeorev.2023.105581

Hubbard, M. J. (2000). Calcium transport across the dental enamel epithelium. *Critical Reviews in Oral Biology and Medicine*, *11*(4), 437–466. https://doi.org/10.1177/10454411000110040401

Hughes, J. M., & Rakovan, J. F. (2015). Structurally robust, chemically diverse: Apatite and apatite supergroup minerals. *Elements*, *11*(3), 165–170. https://doi.org/10.2113/gselements.11.3.165

Humphrey, L. T. (2014). Isotopic and trace element evidence of dietary transitions in early life. *Annals of Human Biology*, *41*(4), 348–357. https://doi.org/10.3109/03014460.2014.923939

Humphrey, L. T., Dean, M. C., Jeffries, T. E., & Penn, M. (2008). Unlocking evidence of early diet from tooth enamel. *Proceedings of the National Academy of Sciences of the United States of America*, *105*(19), 6834–6839. https://doi.org/10.1073/pnas.0711513105

Hurnanen, J., Visnapuu, V., Sillanpää, M., Löyttyniemi, E., & Rautava, J. (2017). Deciduous neonatal line: Width is associated with duration of delivery. *Forensic Science International*, *271*, 87–91. https://doi.org/10.1016/j.forsciint.2016.12.016

ISO. (2016). *ISO 3950:2016 Dentistry — Designation System for Teeth and Areas of the Oral Cavity*. International Organization for Standardization. https://www.iso.org/standard/68292.html

Jensen, S. S., Austin, C., Arora, M., Lie, S. A., Øilo, M., & Klock, K. S. (2023). Toxic and essential trace elements in human primary teeth: A baseline study within The MoBaTooth Biobank and The Norwegian Mother, Father and Child Cohort Study (MoBa). *Environmental Advances*, *13*(July). https://doi.org/10.1016/j.envadv.2023.100418

Jordana, X., Malgosa, A., Casté, B., & Tornero, C. (2019). Lost in transition: the dietary shifts from Late Antiquity to the Early Middle Ages in the North Eastern Iberian Peninsula. *Archaeological and Anthropological Sciences*, *11*(8), 3751–3763. https://doi.org/10.1007/s12520-019-00777-9

Josephsen, K., Takano, Y., Frische, S., Praetorius, J., Nielsen, S., Aoba, T., & Fejerskov, O. (2010). Ion transporters in secretory and cyclically modulating ameloblasts: A new hypothesis for cellular control of preeruptive enamel maturation. *American Journal of Physiology - Cell Physiology*, *299*(6), 1299–1307. https://doi.org/10.1152/ajpcell.00218.2010

Kamenov, G. D., Lofaro, E. M., Goad, G., & Krigbaum, J. (2018). Trace elements in modern and archaeological human teeth: Implications for human metal exposure and enamel diagenetic changes.

Journal of Archaeological Science, *99*(August), 27–34. https://doi.org/10.1016/j.jas.2018.09.002

Kendall, C., Eriksen, A. M. H., Kontopoulos, I., Collins, M. J., & Turner-Walker, G. (2018). Diagenesis of archaeological bone and tooth. *Palaeogeography, Palaeoclimatology, Palaeoecology*, *491*(November 2017), 21–37. https://doi.org/10.1016/j.palaeo.2017.11.041

Kierdorf, H., Witzel, C., Bocaege, E., Richter, T., & Kierdorf, U. (2021). Assessment of physiological disturbances during pre- and early postnatal development based on microscopic analysis of human deciduous teeth from the Late Epipaleolithic site of Shubayqa 1 (Jordan). *American Journal of Physical Anthropology*, *174*(1), 20–34. https://doi.org/10.1002/ajpa.24156

Krachler, M., Rossipal, E., & Micetic-Turk, D. (1999). Trace element transfer from the mother to the newborn - Investigations on triplets of colostrum, maternal and umbilical cord sera. *European Journal of Clinical Nutrition*, *53*(6), 486–494. https://doi.org/10.1038/sj.ejcn.1600781

Kubat, J., Nava, A., Bondioli, L., Dean, M. C., Zanolli, C., Bourgon, N., Bacon, A. M., Demeter, F., Peripoli, B., Albert, R., Lüdecke, T., Hertler, C., Mahoney, P., Kullmer, O., Schrenk, F., & Müller, W. (2023). Dietary strategies of Pleistocene Pongo sp. and Homo erectus on Java (Indonesia). *Nature Ecology and Evolution*, *7*(2), 279–289. https://doi.org/10.1038/s41559-022-01947-0

Kurek, M., Zadzińska, E., Sitek, A., Borowska-Strugińska, B., Rosset, I., & Lorkiewicz, W. (2016). Neonatal line width in deciduous incisors from Neolithic, mediaeval and modern skeletal samples from north-central Poland. *Annals of Anatomy*, *203*, 12–18. https://doi.org/10.1016/j.aanat.2015.02.006

Lacruz, R. S., Habelitz, S., Wright, J. T., & Paine, M. L. (2017). Dental enamel formation and implications for oral health and disease. *Physiological Reviews*, *97*(3), 939–993. https://doi.org/10.1152/physrev.00030.2016

Liu, H., Cui, X., Lu, X., Liu, X., Zhang, L., & Chan, T. S. (2021). Mechanism of Mn incorporation into hydroxyapatite: Insights from SR-XRD, Raman, XAS, and DFT calculation. *Chemical Geology*, *579*(March), 120354. https://doi.org/10.1016/j.chemgeo.2021.120354

Lu, Y., Papagerakis, P., Yamakoshi, Y., Hu, J. C. C., Bartlett, J. D., & Simmer, J. P. (2008). Functions of KLK4 and MMP-20 in dental enamel formation. *Biological Chemistry*, *389*(6), 695–700. https://doi.org/10.1515/BC.2008.080

Lugli, F., Cipriani, A., Capecchi, G., Ricci, S., Boschin, F., Boscato, P., Iacumin, P., Badino, F., Mannino, M. A., Talamo, S., Richards, M. P., Benazzi, S., & Ronchitelli, A. (2019). Strontium and stable isotope evidence of human mobility strategies across the Last Glacial Maximum in southern Italy. *Nature Ecology and Evolution*, *3*(6), 905–911. https://doi.org/10.1038/s41559-019-0900-8

Macchiarelli, R., Bondioli, L., Debénath, A., Mazurier, A., Tournepiche, J. F., Birch, W., & Dean, M. C. (2006). How Neanderthal molar teeth grew. *Nature*, *444*(7120), 748–751. https://doi.org/10.1038/nature05314

Mahoney, P. (2011). Human deciduous mandibular molar incremental enamel development. *American Journal of Physical Anthropology*, *144*(2), 204–214. https://doi.org/10.1002/ajpa.21386

Mahoney, P. (2012). Incremental enamel development in modern human deciduous anterior teeth. *American Journal of Physical Anthropology*, *147*(4), 637–651. https://doi.org/10.1002/ajpa.22029

Mahoney, P. (2015). Dental fast track: Prenatal enamel growth, incisor eruption, and weaning in human infants. *American Journal of Physical Anthropology*, *156*(3), 407–421. https://doi.org/10.1002/ajpa.22666

Martirosyan, A., Sandoval-Ávila, C., Irurita, J., Juanhuix, J., Molist, N., Mestres, I., Durán, M., Alonso, N., Santos, C., Malgosa, A., Molera, J., & Jordana, X. (2024). Reconstructing infant mortality in Iberian Iron Age populations from tooth histology. *Journal of Archaeological Science*, *171*(October). https://doi.org/10.1016/j.jas.2024.106088

Mayer, I., PetÖ, G., Karacs, A., Molnár, G., & Popov, I. (2010). Divalent Mn in calcium hydroxyapatite by pulse laser deposition. *Journal of Inorganic Biochemistry*, *104*(10), 1107–1111. https://doi.org/10.1016/j.jinorgbio.2010.06.009

Mbofung, C. M. F., & Atinmo, T. (1985). Zinc, copper and iron concentrations in the plasma and diets of lactating Nigerian women. *British Journal of Nutrition*, *53*(3), 427–439. https://doi.org/10.1079/bjn19850052

McFarlane, G., Loch, C., Guatelli-Steinberg, D., Bayle, P., Le Luyer, M., Sabel, N., Nava, A., Floyd, B., Skinner, M., White, S., Pitfield, R., & Mahoney, P. (2021). Enamel daily secretion rates of deciduous molars from a global sample of children. *Archives of Oral Biology*, *132*(September), 105290. https://doi.org/10.1016/j.archoralbio.2021.105290

Micó, C., Blasco, R., & Rivals, F. (2024). Simulating taphonomic processes on teeth: The impact of sediment pressure and thermal alteration on dental microwear. *Quaternary Science Advances*, *14*(March). https://doi.org/10.1016/j.qsa.2024.100195

Müller, W., Lugli, F., McCormack, J., Evans, D., Anczkiewicz, R., Bondioli, L., & Nava, A. (2024). Human life histories. In *Reference Module in Earth Systems and Environmental Sciences*. Elsevier Inc. https://doi.org/10.1016/b978-0-323-99762-1.00105-4

Müller, W., Nava, A., Evans, D., Rossi, P. F., Alt, K. W., & Bondioli, L. (2019). Enamel mineralization and compositional time-resolution in human teeth evaluated via histologically-defined LA-ICPMS profiles. *Geochimica et Cosmochimica Acta*, *255*, 105–126. https://doi.org/10.1016/j.gca.2019.03.005

Nanci, A. (2018). Ten Cate's Oral Histology - E-Book: Develpment, Structure and Function. *Structure of the Oral Tissues*, 1–13.

Nava, A., Coppa, A., Coppola, D., Mancini, L., Dreossi, Di., Zanini, F., Bernardini, F., Tuniz, C., & Bondioli, L. (2017). Virtual histological assessment of the prenatal life history and age at death of the

Upper Paleolithic fetus from Ostuni (Italy). *Scientific Reports*, *7*(1), 1–10. https://doi.org/10.1038/s41598-017-09773-2

Nava, A., Lugli, F., Lemmers, S., Cerrito, P., Mahoney, P., Bondioli, L., & Müller, W. (2024). Reading children's teeth to reconstruct life history and the evolution of human cooperation and cognition: The role of dental enamel microstructure and chemistry. *Neuroscience and Biobehavioral Reviews*, *163*(February), 105745. https://doi.org/10.1016/j.neubiorev.2024.105745

Nava, A., Lugli, F., Romandini, M., Badino, F., Evans, D., Helbling, A. H., Oxilia, G., Arrighi, S., Bortolini, E., Delpiano, D., Duches, R., Figus, C., Livraghi, A., Marciani, G., Silvestrini, S., Cipriani, A., Giovanardi, T., Pini, R., Tuniz, C., … Benazzi, S. (2020). Early life of Neanderthals. *Proceedings of the National Academy of Sciences of the United States of America*, *117*(46), 28719–28726. https://doi.org/10.1073/pnas.2011765117

Pajor, K., Pajchel, L., & Kolmas, J. (2019). Hydroxyapatite and fluorapatite in conservative dentistry and oral implantology-a review. *Materials*, *12*(7). https://doi.org/10.3390/ma12172683

Peripoli, B., Gigante, M., Mahoney, P., McFarlane, G., Coppa, A., Lugli, F., Lauria, G., Bondioli, L., Sconzo, P., Sineo, L., & Nava, A. (2023). Exploring prenatal and neonatal life history through dental histology in infants from the Phoenician necropolis of Motya (7th–6th century BCE). *Journal of Archaeological Science: Reports*, *49*(February), 104024. https://doi.org/10.1016/j.jasrep.2023.104024

R Core Team. (2022). *R: A Language and Environment for Statistical Computing (Version 4.2.0)*. R Foundation for Statistical Computing.

Rey, L., Tacail, T., Santos, F., Rottier, S., Goude, G., & Balter, V. (2022). Disentangling diagenetic and biogenic trace elements and Sr radiogenic isotopes in fossil dental enamel using laser ablation analysis. *Chemical Geology*, *587*(September 2021). https://doi.org/10.1016/j.chemgeo.2021.120608

Sabel, N., Johansson, C., Kühnisch, J., Robertson, A., Steiniger, F., Norén, J. G., Klingberg, G., & Nietzsche, S. (2008). Neonatal lines in the enamel of primary teeth-A morphological and scanning electron microscopic investigation. *Archives of Oral Biology*, *53*(10), 954–963. https://doi.org/10.1016/j.archoralbio.2008.05.003

Saito, K., Kagawa, S., Ogasawara, M., & Kato, S. (2023). Multiple incorporation of copper and iron ions into the channel of hydroxyapatite. *Journal of Solid State Chemistry*, *317*(August 2022), 123673. https://doi.org/10.1016/j.jssc.2022.123673

Sarna-Boś, K., Boguta, P., Skic, K., Wiącek, D., Maksymiuk, P., Sobieszczański, J., & Chałas, R. (2022). Physicochemical Properties and Surface Characteristics of Ground Human Teeth. *Molecules*, *27*(18). https://doi.org/10.3390/molecules27185852

Sarna-Boś, K., Skic, K., Boguta, P., Adamczuk, A., Vodanovic, M., & Chałas, R. (2023). Elemental mapping of human teeth enamel, dentine and cementum in view of their microstructure. *Micron*, *172*(March). https://doi.org/10.1016/j.micron.2023.103485

Schindelin, J., Arganda-Carreras, I., Frise, E., Kaynig, V., Longair, M., Pietzsch, T., Preibisch, S., Rueden, C., Saalfeld, S., Schmid, B., Tinevez, J. Y., White, D. J., Hartenstein, V., Eliceiri, K., Tomancak, P., & Cardona, A. (2012). Fiji: An open-source platform for biological-image analysis. *Nature Methods*, *9*(7), 676–682. https://doi.org/10.1038/nmeth.2019

Shaik, I., Dasari, B., SHaik, A., Doos, M., Kolli, H., Rana, D., & Tiwari, R. (2021). Functional Role of Inorganic Trace Elements on Enamel and Dentin Formation: A Review. *Journal of Pharmacy And Bioallied Sciences*, *13(Suppl 2*, S952–S956. https://doi.org/10.4103/jpbs.jpbs_392_21

Sharma, V., Rastogi, S., Bhati, K. K., Srinivasan, A., Roychoudhury, A., Nikolajeff, F., & Kumar, S. (2020). Mapping the inorganic and proteomic differences among different types of human teeth: A preliminary compositional insight. *Biomolecules*, *10*(11), 1–16. https://doi.org/10.3390/biom10111540

Simmer, J. P., Hu, Y., Richardson, A. S., Bartlett, J. D., & Hu, J. C. C. (2011). Why does enamel in Klk4-null mice break above the dentino-enamel junction? *Cells Tissues Organs*, *194*(2–4), 211–215. https://doi.org/10.1159/000324260

Simmer, J. P., Richardson, A. S., Hu, Y. Y., Smith, C. E., & Ching-Chun Hu, J. (2012). A post-classical theory of enamel biomineralization and why we need one. *International Journal of Oral Science*, *4*(3), 129–134. https://doi.org/10.1038/ijos.2012.59

Smith, T. M., Arora, M., Bharatiya, M., Dirks, W., & Austin, C. (2023). Elemental models of primate nursing and weaning revisited. *American Journal of Biological Anthropology*, *180*(1), 216–223. https://doi.org/10.1002/ajpa.24655

Smith, T. M., Austin, C., Ávila, J. N., Dirks, W., Green, D. R., Williams, I. S., & Arora, M. (2022). Permanent signatures of birth and nursing initiation are chemically recorded in teeth. *Journal of Archaeological Science*, *140*(February). https://doi.org/10.1016/j.jas.2022.105564

Solé, V. A., Papillon, E., Cotte, M., Walter, P., & Susini, J. (2007). A multiplatform code for the analysis of energy-dispersive X-ray fluorescence spectra. *Spectrochimica Acta - Part B Atomic Spectroscopy*, *62*(1), 63–68. https://doi.org/10.1016/j.sab.2006.12.002

Specht, A. J., Zhang, X., Antipova, O. A., Sayam, A. S. M., Nguyen, V. T., Hoover, C. G., Punshon, T., Jackson, B. P., & Weisskopf, M. G. (2025). Sub-micrometer scale synchrotron X-ray fluorescence measurements of trace elements in teeth compared with laser ablation inductively coupled plasma mass spectrometry. *Journal of Exposure Science & Environmental Epidemiology*. https://doi.org/10.1038/s41370-025-00754-6

Stimmler, L., Snodgrass, G. J. A. ., & Jaffe, E. (1973). Dental defects associated with neonatal symptomatic hypocalcaemia. *Archives of Disease in Childhood*, *48*(0), 217–220.

Subirà, M. E., & Molist, N. (2007). Inhumacions perinatals múltiples i espais de treball en els assentaments ibers. *Nasciturus: Infans, Puerulus. Vobis Mater Terra. La Muerte En La Infancia*, *Uh 4*, 365–385.

Tamura, Y., George, M., & Goyer, A. (n.d.). *Preanancv-Associated Chanaes*. *43553*.

Terrin, G., Canani, R. B., Di Chiara, M., Pietravalle, A., Aleandri, V., Conte, F., & De Curtis, M. (2015). Zinc in early life: A key element in the fetus and preterm neonate. *Nutrients*, *7*(12), 10427–10446. https://doi.org/10.3390/nu7125542

Wasowicz, W., Gromadzinska, J., Szram, K., Rydzynski, K., Cieslak, J., & Pietrzak, Z. (2001). Selenium, zinc, and copper concentrations in the blood and milk of lactating women. *Biological Trace Element Research*, *79*(3), 221–233. https://doi.org/10.1385/BTER:79:3:221

Williams, A. M. M., & Siegele, R. (2014). Iron deposition in modern and archaeological teeth. *Nuclear Instruments and Methods in Physics Research, Section B: Beam Interactions with Materials and Atoms*, *335*, 19–23. https://doi.org/10.1016/j.nimb.2014.06.003

Witzel, C., Kierdorf, U., Schultz, M., & Kierdorf, H. (2008). Insights from the inside: Histological analysis of abnormal enamel microstructure associated with hypoplastic enamel defects in human teeth. *American Journal of Physical Anthropology*, *136*(4), 400–414. https://doi.org/10.1002/ajpa.20822

Zanolli, C., Bondioli, L., Manni, F., Rossi, P., & Macchiarelli, R. (2011). Gestation length, mode of delivery, and neonatal line-thickness variation. *Human Biology*, *83*(6), 695–713. https://doi.org/10.3378/027.083.0603

Zheng L, Ehardt L, McAlpin B et al. (2014) The tick tock of odontogenesis. Experimental Cell Research 325(2):83-89. https://doi.org/10.1016/j.bone.2013.02.011

Zheng L, Seon YJ, Mourão MA et al. (2013) Circadian rhythms regulate amelogenesis. Bone 55(1):158-165.